

# Numerical Analysis on Effect of Permeability and Reinforcement Length (Drainage Path) in Reinforced Soil

## 보강토에서의 투수성과 보강재길이(배수거리)의 영향에 대한 수치해석

Lee, Hong-Sung<sup>†</sup> · Hwang, Young-Cheol<sup>1)</sup>

이 흥 성 · 황 영 철

**ABSTRACT :** Excess pore pressures in low permeability soils may not dissipate quickly enough and decrease the effective stresses inside the soil, which in turn may cause a reduction of the shear strength at the interface between the soil and the reinforcement in MSE walls. For this condition the dissipation rate of pore pressures is most important and it varies depending on wall size, permeability of the backfill, and reinforcement length. In this paper, a series of numerical analysis has been performed to investigate the effect of those factors. The results show that for soils with a permeability lower than  $10^{-3}$  cm/sec, the consolidation time gradually increases. The increase in consolidation time indicates the decrease in effective stress thus it will result in decrease in pullout capacity of the reinforcement as verified by the numerical analyses. It is also observed that larger consolidation time is required for longer reinforcement length (longer drainage path).

**Keywords :** Excess pore pressure, MSE wall, Permeability, Reinforcement length, Drainage path

**요 지 :** 투수성이 낮은 흙에서 과잉간극수압은 빨리 소산되지 못하므로 유효응력을 감소시키게 되며, 이는 보강토 옹벽에서 보강재와 흙 사이의 인터페이스 전단강도를 감소시키는 결과를 가져온다. 이러한 조건에서는 간극수압의 소산속도가 매우 중요하며, 이는 벽체의 크기, 뒤채움 흙의 투수성 그리고 보강재의 길이 등에 의해 영향을 받는다. 본 논문에서는 이러한 영향요소의 효과를 조사하기 위하여 유한요소해석을 실시하였고, 그 결과 투수계수  $10^{-3}$ cm/sec 이하부터는 간극수압 소산시간이 점차 증가하기 시작함을 알 수 있었다. 간극수압 소산시간의 증가는 유효응력의 감소를 의미하여 보강재 인발력의 감소로 이어질 것이며, 이는 본 논문에서 수행된 수치해석으로 확인되었다. 또한, 보강재의 길이가 길수록 간극수압 소산시간이 더 많이 필요한 것으로 나타났는데 이는 배수거리의 증가에 기인한다.

**주요어 :** 과잉간극수압, 보강토 옹벽, 투수성, 보강재 길이, 배수거리

## 1. Introduction

Since Vidal (1969), a French engineer, developed the modern concept of MSE walls, the use of Mechanically Stabilized Earth (MSE) retaining walls has increased dramatically in civil engineering projects. MSE walls are used as design alternatives to traditional reinforced concrete retaining walls because of their capability to retain earth fills of significant height and sustain surface applied loads at lower cost than reinforced concrete walls. In general, MSE walls consist of a structural fill reinforced with tensile-resistant inclusions that are connected to facing elements. MSE walls are internally stabilized through mechanical interaction between three components: backfill, reinforcement, and facing.

The current design of MSE walls is based on limit state analysis where the ultimate strength of the soil and the pullout capacity of the reinforcement are considered. This has been applied to drained conditions. The behavior of MSE walls in drained and undrained conditions is quite different, especially when fine grain soils or granular soils with fines are used as backfill. The stability of MSE walls with such backfill may be compromised in undrained conditions which may occur during heavy rain or during a rapid draw-down. Excess pore pressures in low permeability soils may not dissipate quickly enough and decrease the effective stresses inside the soil, which in turn may cause a reduction of the shear strength at the interface between the soil and the reinforcement. Study of MSE walls in undrained conditions

<sup>†</sup> Member, Senior Researcher, Hyundai Engineering & Construction Co., LTD(E-mail : hongsung@hdec.co.kr)

<sup>1)</sup> Member, Assistant Professor, Sangji University

is needed to determine the behavior of saturated MSE walls where rapid changes in pore pressures are anticipated.

In undrained condition, the normal effective stress decreases and the pullout capacity decreases with increasing pore pressures. As the pore pressures generated dissipate, the effective stress increases and the pullout capacity increases; thus the dissipation rate of pore pressures is an important factor. The permeability and the distance from a given point in the soil to the closest drainage boundary govern the time that will take for the pore pressures to dissipate. The time for pore pressure dissipation defines whether drained or undrained conditions occur. For example, if a section of the wall is submerged during flooding, undrained conditions within the soil will be generated if the water level decreases at a rate faster than the pore pressures inside the wall are dissipated. The dissipation time of pore pressures varies depending on wall size, permeability of the backfill, and reinforcement length. In this paper, a series of numerical analysis has been performed to investigate the effect of those factors. The Finite Element (FE) program, ABAQUS (1999) is used for the investigation. ABAQUS is a general-purpose FE software that is very well suited for this analysis since it can incorporate a coupled mechanical analysis with pore pressure dissipation in porous-elastic materials.

## 2. Numerical Analysis (No Reinforcement)

### 2.1 Dimensions of the Model

The dimensions of the model used for the 2D numerical

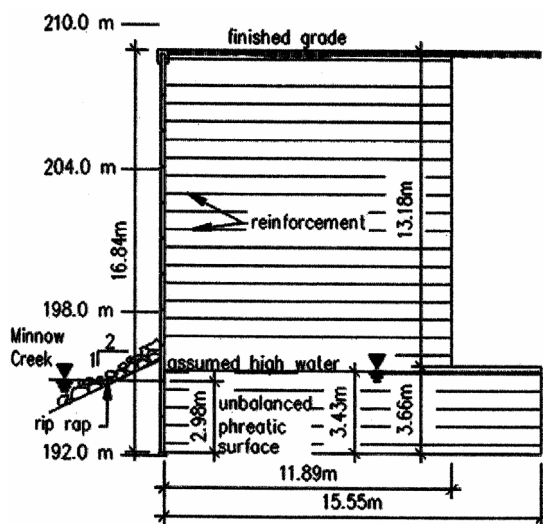


Fig. 1. Minnow creek wall (Runser, 1999)

analysis have been obtained from the Minnow Creek Wall (Runser, 1999), which is 17 m tall, the tallest MSE wall built in Indiana, U.S.A. as of 1999 (see Figure 1). As shown in the figure, the longest reinforcement is 15.55 m long, and is placed at the bottom of the wall. The reinforcements are spaced vertically at 0.75 m. During a rapid drawdown, dissipation of pore pressures occurs both upwards and towards the facing of the wall.

Because of the constant spacing of the reinforcement, the volume of soil matrix with unit width modeled is that between two layers of reinforcement. Based on the wall dimensions and drainage conditions, a basic model for the analysis is taken as 16 m long and 0.75 m high with a vertical load corresponding to the weight of the 17 m backfill, as shown in Figure 2. In addition, the length of the reinforcement (i.e. drainage length) is varied to investigate the effect of wall size. It is also assumed that the length of the backfill is the same as that of the reinforcement.

### 2.2 Boundary Conditions

Figure 3 shows the boundary conditions of the finite element model. Both the left and right sides of the model are supported by rollers allowing vertical displacements.

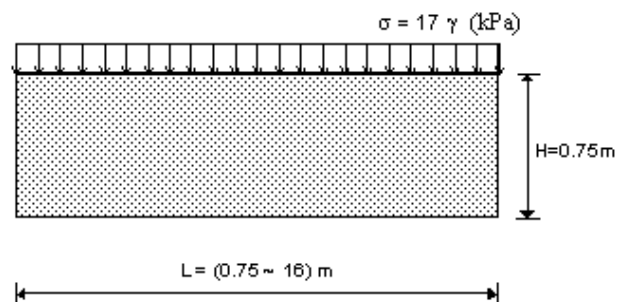


Fig. 2. Dimensions of the soil matrix for numerical analysis

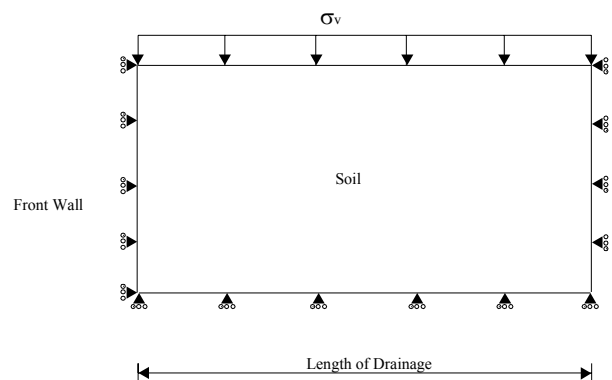


Fig. 3. Boundary conditions at the bottom of the wall (side view)

Horizontal displacements are not allowed on the sides of the model to reproduce the initial geostatic,  $K_0$ , loading conditions. Horizontal displacements are allowed at the bottom of the model by rollers and vertical displacements are constrained.

### 2.3 Mesh Formation and Element Selection

Since the purpose of the analysis is to investigate the dissipation rate of pore pressures, only the soil is modeled; reinforcement is not modeled. Although the elements are not shown in Figure 3, the size of the soil elements range from 0.075 m to 0.25 m horizontal, and 0.075 m vertical depending on the total length of the model. The total number of elements is about 2000. As a result of a few trials with different mesh formation, it has been found that the mesh formation for this analysis is well refined and the model is properly simulated.

Retaining walls are the structures that can be considered very long in the dimension perpendicular to the cross section; thus plane strain conditions can be assumed. Because of that, all elements in the model are 8-node biquadratic plane strain elements, with pore pressure at the corner nodes (CPE8P, from the ABAQUS element library). All nodes have two degrees of freedom: horizontal and vertical displacements; the corner nodes have pore pressures as an additional degree of freedom.

### 2.4 Initial Stresses

The numerical analysis was executed in two stages. In the first stage, the initial loading conditions were applied. This was done by imposing a vertical stress to the top of the mesh, corresponding to the self-weight of the 17 m backfill. In this stage,  $K_0$  conditions are reached since lateral movements are prevented and no excess pore pressures are generated (i.e. the vertical,  $\sigma_v$ , and horizontal stresses,  $\sigma_h = K_0 \times \sigma_v$  are effective stresses). The soil is fully saturated and the water level is at the top of the mesh. In the second stage, the pore pressures at the top and left hand sides of the mesh are set to zero (i.e. rapid drawdown with drainage along these two sides), and pore pressures begin to dissipate as drainage of the water occurs through the top and left sides of the model. Consolidation is allowed until 95% of dissipation of pore pressure is obtained throughout the

entire mesh.

## 2.5 Material Properties

With the properties of the clean sand used in the pullout tests (Lee and Bobet, 2005), the soil is modeled as an elastic material because the soil would behave within elastic range in this analysis. Among the properties, Young's Modulus and Poisson's ratio are estimated as 30 MPa and 0.25, respectively. The coefficient of lateral earth pressure is 0.4 and the initial void ratio is 0.52. Table 1 summarizes the material properties.

## 2.6 Variables Investigated

Two variables are investigated in this analysis: (1) permeability; and (2) length of reinforcement. The coefficients of permeability selected for the analysis range from  $10^{-1}$  cm/sec to  $10^{-4}$  cm/sec, which cover the range of permeabilities of the materials tested (Lee and Bobet, 2005). A total of 4 permeabilities are analyzed:  $10^{-1}$ ,  $10^{-2}$ ,  $10^{-3}$ , and  $10^{-4}$  cm/sec, and six reinforcement lengths: 0.75, 2, 4, 8, 12, and 16 m. The height of the wall is kept constant at 0.75 m, which is the standard reinforcement spacing used in practice. Table 2 shows the values of the variables investigated.

## 3. Preliminary Analysis

A preliminary analysis is performed to verify the model. A comparison between a 1-D analysis with ABAQUS and closed-form solutions is made. The FE model for the verification is the same model described in previous sections, except that the model has a unit width and dissipation of

Table 1. Material Properties of the Soil

Young's Modulus (MPa)	Poisson's Ratio	Coefficient of Lateral Earth Pressure	Initial Void Ratio
30	0.25	0.4	0.52

Table 2. Variables Investigated

Coefficient of Permeability (cm/sec)	Length of Reinforcement (m)
$10^{-1}$	0.75, 2, 4, 8, 12, and 16
$10^{-2}$	0.75, 2, 4, 8, 12, and 16
$10^{-3}$	0.75, 2, 4, 8, 12, and 16
$10^{-4}$	0.75, 2, 4, 8, 12, and 16

pore pressure occurs through the top boundary only. The permeability used is  $10^{-1}$  cm/sec.

The closed-form solution is based on Terzaghi's theory of 1-D consolidation. The time factor ( $T_v$ ) for a certain degree of consolidation ( $U$ ) is obtained using Equation 1. For the analysis, the target degree of consolidation is 95%, and consequently, the time factor is 1.129 (i.e.  $T_v = 1.129$ ).

$$T_v = 1.781 - 0.933 \log(100 - U\%) \quad \text{for } U > 60\% \quad (\text{Eq. 1})$$

Equation 2 is used to obtain  $c_v$ , the coefficient of consolidation.

$$c_v = \frac{k}{m_v \cdot \gamma_w} \quad (\text{Eq. 2})$$

where,  $k$  = permeability ( $10^{-3}$  m/sec)

$\gamma_w$  = unit weight of water ( $9.81$  kN/m<sup>3</sup>)

$m_v$  = coefficient of volume change

$$= \frac{(1 + \nu)(1 - 2\nu)}{E(1 - \nu)}$$

Equation 3 is used to obtain  $t_{95}$ , the time required for 95% of consolidation. With the material properties,  $c_v = 3.67$  m<sup>2</sup>/sec obtained using Equation 2, and with the model geometry,  $H_{dr} = 0.75$  m, this results in  $t_{95} = 0.173$  seconds.

$$T_{95} = \frac{c_v \cdot t_{95}}{H_{dr}^2} \quad (\text{Eq. 3})$$

where,  $c_v$  = coefficient of consolidation

$t_{95}$  = 95% consolidation time

$H_{dr}$  = average longest drainage path during consolidation

With ABAQUS, 0.185 seconds are needed for 95% consolidation, as shown in Figure 4. The difference is about

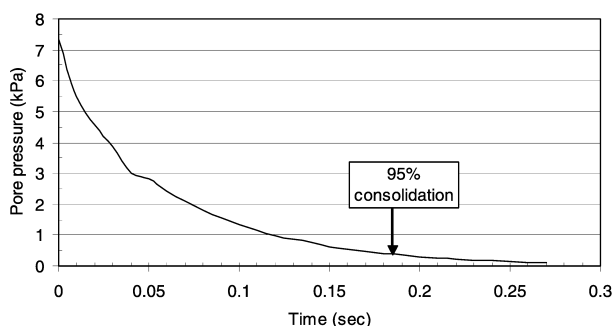


Fig. 4. Result of Preliminary Analysis for 1-D Consolidation

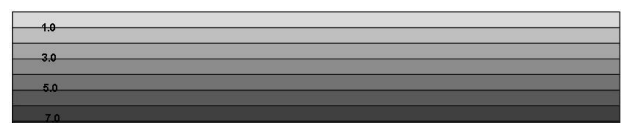
6%, which is small enough for practical purposes.

## 4. Results of Numerical Analysis (No Reinforcement)

The pore pressures will dissipate at different rates throughout the model depending on the distance to a drainage boundary; the nearer to the boundary, the more quickly the pore pressures dissipate. The point at the bottom right corner of the mesh (Figure 3) is taken as a reference to evaluate the dissipation of the pore pressures. This is the farthest point from the drainage boundaries, and thus if 95% of pore pressures have dissipated at this point, the dissipation of excess pore pressures will be smaller in the rest of the model (i.e. dissipation will be higher than 95% in the rest of the model).

### 4.1 Pore Pressure Distribution

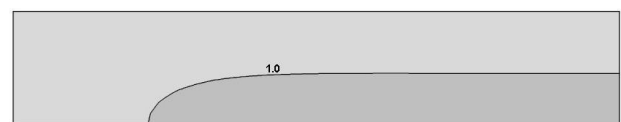
To investigate the dissipation and distribution of pore pressures throughout the model, detailed plots are presented for one particular case. The case corresponds to a soil with permeability  $10^{-2}$  cm/sec and a reinforcement length of 4 m. Figure 5 (a) shows the pore pressure distributions at the beginning of the analysis (i.e. end of stage 1 or initial/geostatic



(a)  $t = 0$  sec



(b)  $t = 0.2$  sec



(c)  $t = 1.0$  sec



(d)  $t = 1.9$  sec

Fig. 5. Pore pressure distribution (unit : kPa)

conditions). As one can observe in the figure, the pore pressure distribution is linear with depth (i.e. hydrostatic), with a maximum of 7.36 kPa, which corresponds to a column of water of 0.75 m. Figures 5 (b) to (d) show the pore pressure distribution with time. Note that in the figures the top and left boundaries are drainage boundaries where the pore pressures are zero. The plots show that dissipation occurs very rapidly on the left hand side and quickly progresses to the bottom and right sides of the model. After only 0.2 seconds, 40% of consolidation has already occurred at the reference point (bottom right corner of the mesh). A 95% pore pressure dissipation occurs at 1.9 seconds. The plots also show how the pore pressure contours adapt to the shape of the boundaries: the vertical contours are parallel to the left side and the horizontal are parallel to the top. This indicates how dissipation progresses towards the drainage boundaries.

## 4.2 Effect of Permeability and Reinforcement Length

Consolidation time increases as the permeability decreases. Figure 6 shows results of 95% consolidation time for different reinforcement lengths and permeabilities. Permeability has a dramatic effect on the time that takes for the pore pressures to dissipate. For permeabilities larger than  $10^{-2}$  cm/sec, dissipation of pore pressures is almost immediate. As the permeability decreases below  $10^{-2}$  cm/sec, the time required for 95% consolidation begins to increase, and it increases dramatically if the permeability is smaller than  $10^{-3}$  cm/sec.

Figure 6 shows that the length of reinforcement does not affect much the time for consolidation for permeabilities

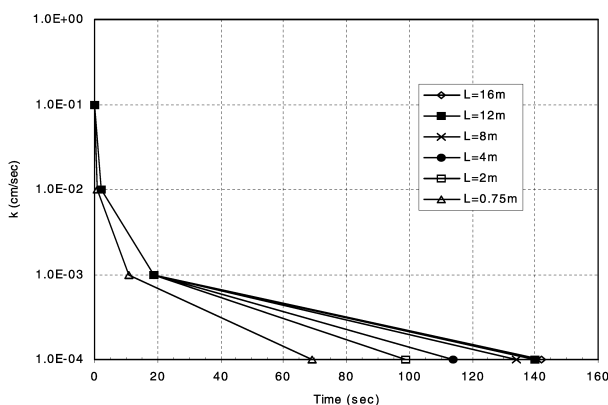


Fig. 6. Results of numerical analysis; Effect of permeability and reinforcement length

above  $10^{-2}$  cm/sec. For permeabilities between  $10^{-2}$  cm/sec and  $10^{-3}$  cm/sec the results are independent of the reinforcement length except for the case of reinforcement length 0.75 m. This indicates that for larger reinforcements the drainage path is mostly towards the upper boundary, which is located 0.75 m above the reference point. As expected, the consolidation time decreases as drainage increases in the two directions. For permeabilities lower than  $10^{-3}$  cm/sec, the consolidation time increases and the influence of the reinforcement length is larger.

## 5. Effect of Permeability on Pullout Capacity (Numerical Analysis with Reinforcement)

### 5.1 Modelling of Numerical Analysis

A series of 2D numerical analysis has been performed varying permeability in order to investigate the effect of permeability on pullout capacity. Figure 7 shows a boundary condition used in the analysis. Initial conditions including boundary condition are the same as the ones in previous analysis (See Fig. 3) except for the dimensions, overburden pressure and placement of steel reinforcement. Dimensions of the soil matrix and steel reinforcement have been obtained from the dimensions of laboratory pullout tests (Lee and Bobet, 2005); the dimensions of the pullout box and steel reinforcement are 1 m (length) and 0.2 m (height) for the pullout box, and 0.75 m (length) and 3 mm (thickness) for the reinforcement. Since the analysis is performed symmetrically, only the half thickness of the reinforcement is modeled (1.5 mm) in this analysis. Also, self weight of the soil is neglected. An overburden pressure of 30 kPa is applied on top of the box. A clean sand was used for the analysis in

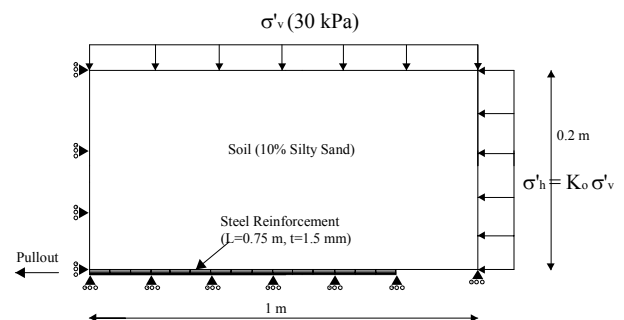


Fig. 7. Boundary conditions

the previous section while a 10% silty sand (i.e. 10% silt contents in weight) is used as backfill material in this section because the reduction in pullout capacity is more significant for low permeability soil. It should be noted that dissipation of excessive pore pressure occurs towards the top boundary and left boundary. For steel reinforcement element, 8-node biquadratic plane strain elements are used (CPE8, from the ABAQUS element library). An element of INTER3P is used for the interface between soil and reinforcement.

Material properties used in the analysis are summarized in Table 3. In this analysis, a silty sand was used, while clean sand was used in previous section, because undrained behavior is more distinct in low permeability soil, a silty sand, than in clean sand. Basic properties of the soil have been obtained from the results of triaxial tests performed by Salgado et al. (2000). Since the purpose of the analysis is to investigate the effect of permeability, different coefficients of permeability have been used from dry condition to  $3.83 \times 10^{-5}$  cm/sec. A permeability of  $3.83 \times 10^{-3}$  cm/sec is denoted as  $k_1$ ,  $3.83 \times 10^{-4}$  cm/sec is  $k_2$ , which is 10 times smaller than  $k_1$ , and  $3.83 \times 10^{-5}$  cm/sec is denoted as  $k_3$ , which is 10 times smaller than  $k_2$  and 100 times smaller than  $k_1$ . Young's Modulus of steel reinforcement is 210,000 MPa and poisson's ratio is 0.3.

## 5.2 Results of Analysis

Figure 8 shows the results of numerical analysis on effect of permeability. The pullout capacity is obtained when the interface shear strength reaches to the pre-determined coefficient of interface friction. As shown in the figure, pullout capacity decreases as permeability decreases; 2.1 kPa for dry condition, 2.01 kPa for permeability  $k_1$ , 1.7 kPa for permeability  $k_2$ , and 1.1 kPa for permeability  $k_3$ . This is due to that interface shear strength between reinforcement and soil decreases resulting from reduction of

effective stress acting on the reinforcement. In addition, the pullout capacity ratio, which is a ratio of pullout capacity for each permeability to pullout capacity for dry condition, also decreases from 100% (dry condition) to 52.4% (permeability  $k_3$ ). The reduction in the ratio increases as the permeability decreases. This result shows a good agreement with the results in previous section, where the dissipation time increases as permeability decreases, resulting in decrease of effective stress thus decrease of pullout capacity. The reduction ratio between dry condition and permeability  $k_1$  is not large because the drainage path is short in this analysis. Because of the short drainage path (0.2 m in vertical direction), excessive pore pressure dissipates relatively quickly. However, reduction is significant from permeability  $k_2$  in spite of short drainage path.

Based on the results of the numerical analysis, it is recommended that use of soils with permeability smaller than  $3.83 \times 10^{-4}$  cm/sec should be avoided as backfill material because significant reduction in pullout capacity is anticipated. Since in-situ drainage path is generally longer than the one in this analysis, dissipation time is longer for the same permeability. It is, therefore, more conservative to avoid the use of soils with permeability smaller than  $10^{-3}$  cm/sec where consolidation time significantly increases as obtained in Chapter 4. In addition, it should be noted that the results obtained from this paper may be different from in-situ

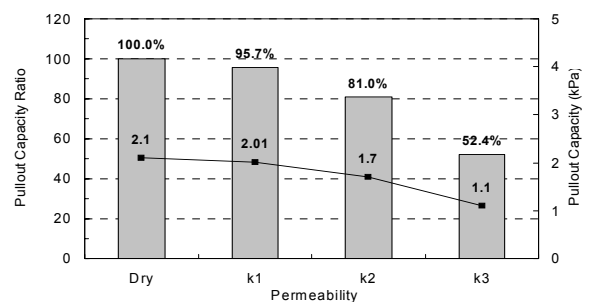


Fig. 8. Results of numerical analysis: Effect of permeability on pullout capacity

Table 3. Material properties of the soil

Young's Modulus (MPa)	Poisson's Ratio	Coefficient of Lateral Earth Pressure (K)	Peak Friction Angle (°)	Coefficient of Interface Friction	Permeability (cm/sec)
40	0.25	0.412	45.5	0.588	Dry condition, $3.83 \times 10^{-3}$ , ( $k_1$ ) $3.83 \times 10^{-4}$ , ( $k_2$ ) $3.83 \times 10^{-5}$ , ( $k_3$ )

performance because of installation of filtering materials in MSE walls.

More comprehensive analyses on drained and undrained pullout capacity in reinforced soil have been performed by the author, and the results are published in another paper (Lee and Son, 2007). For more information on numerical modeling and its results, readers are advised to refer to the paper.

## 6. Conclusions

It has been found from the numerical analyses that the dissipation of pore pressures is very fast for permeabilities larger than  $10^{-3}$  cm/sec. Because of the quick dissipation, it is expected that the pullout capacity for soils with permeability larger than  $10^{-2}$  cm/sec will not change much with drainage conditions. For a permeability of  $10^{-3}$  cm/sec, the dissipation of pore pressures becomes slower depending on length of drainage path, and it becomes significantly slow for a permeability of  $10^{-4}$  cm/sec. Thus for soils with a permeability lower than  $10^{-3}$  cm/sec, the pullout capacity in saturated soils should be much smaller than the pullout capacity in dry condition, resulting from decrease in effective stress.

It is well known that the pullout capacities in saturated soils with high permeability are the same as the pullout capacities in dry condition, which indicates that excess pore pressures do not have any influence. However, the pullout capacity in saturated soils with low permeability will be smaller than the pullout capacity in dry condition. Numerical analyses have been performed to investigate the

effect of permeability on pullout capacity. The results of the analyses show that as the permeability decreases the pullout capacity decreases relative to the pullout capacity for dry condition; the ratio is 96% for permeability of  $3.83 \times 10^{-3}$  cm/sec, 81% for permeability of  $3.83 \times 10^{-4}$  cm/sec, and 52% for permeability of  $3.83 \times 10^{-5}$  cm/sec.

Based on these results, it can be concluded that if the permeability is small enough so the excess pore pressures have no time to dissipate, the pullout capacity decreases dramatically. Therefore, appropriate design should be conducted when the soils with low permeability are used as backfill of the MSE walls.

## References

1. Abaqus Manual (1999), Hibbit, Karlson & Sorenson, Inc.
2. Lee, H. S. and Bobet, A. (2005), *Laboratory evaluation of pullout capacity of reinforced silty sands in drained and undrained condition*, ASTM Geotechnical Testing Journal, Vol. 28, No. 4, pp. 370~379.
3. Lee, H. S. and Son, M. (2007), *Numerical analysis on drained and undrained pullout capacity in reinforced soil*, Journal of the Korean Geotechnical Society, Vol. 23, No. 4, pp. 113~123 (in Korean).
4. Runser, D. J. (1999), *Instrumentation and experimental evaluation of a 17 m tall reinforced earth retaining wall*, MS thesis, Purdue University, pp. 52.
5. Salgado, R., Bandini, P. and Karim, A. (2000), *Shear Strength and Stiffness of Silty Sand*, Journal of Geotech and Geoenvironmental Eng. Div. ASCE, Vol. 126, Issue 5, pp. 451~462.
6. Vidal, H. (1969), *The Principle of Reinforced Earth*, Transportation Research Record, 282, pp. 1~16.

(접수일: 2007. 3. 23 심사일: 2007. 4. 20 심사완료일: 2007. 5. 22)